The concrete columns as a sensible thermal energy storage medium and a heater

ARTICLE *in* HEAT AND MASS TRANSFER · FEBRUARY 2014

Impact Factor: 0.95 · DOI: 10.1007/s00231-014-1313-5

2 AUTHORS, INCLUDING:

Sebahattin Ünalan
Erciyes Üniversitesi
18 PUBLICATIONS **78** CITATIONS

The concrete columns as a sensible thermal energy storage medium and a heater

Sebahattin Ünalan & Evrim Özrahat

Heat and Mass Transfer
Wärme- und Stoffübertragung

ISSN 0947-7411

Heat Mass Transfer
DOI 10.1007/s00231-014-1313-5

Springer

Heat Mass Transfer
DOI 10.1007/s00231-014-1313-5

ORIGINAL

The concrete columns as a sensible thermal energy storage medium and a heater

Sebahattin Ünalan · Evrim Özrahat

Received: 19 July 2011 / Accepted: 24 February 2014

Abstract This study investigated storage possibility of sensible thermal energy in the concrete columns of multi-storey buildings and the heating performance of the indoors with the stored energy. In the suggested system, the dry air heated in an energy center will be circulated in stainless steel pipes through columns. The sensible thermal energy would firstly be stored by means of forced convection in column medium. Then, the stored thermal energy will transfer by natural convection and radiation from the column surfaces to indoor spaces. The transient thermal calculations are realized for a flat of the 11-storey building in Kayseri city of Turkey. The thermal energy requirement of the flat is nearby 5.3 kW as an average of a winter season. The simplified transient calculations were carried out over a concrete hollow cylindrical column having outer radius of 0.31 m and inner radius of 0.05 m corresponding an averaged column section in the sample flat. The flow temperature was selected between T = 350 and 500 K, which are considerably lower than the temperature of 573 K assumed as a limit for thermal strength of the concrete in the literature. The flow velocity ranges were selected between V = 1.0 and 5.0 m/s. The initial temperature was assumed as 293 K. After the first energy charging process of 23 h, for T = 350 K and V = 1.0 m/s, the total heat flux from the column surfaces into indoors are nearby 5.5 kW. The first charging time required to reach the energy requirement of 5.3 kW is decreased by increasing the flow velocity and temperature. Also for 5.0 m/s–350 K and 5.0 m/s–450 K, this time can decrease to 10 and 4.5 h, respectively. In addition, with 4.0 m/s–360 K or 2.0 m/s–400 K, after the energy charging of 8 h, the energy requirement of 5.3 kW can be provided by the energy discharging of 16 h and the energy charging of 8 h during 7 days. The results are very attractive in terms of the building heating systems of the future.

S. Ünalan (✉)
Department of Mechanical Engineering, Faculty of Engineering, University of Erciyes, 38039 Melikgazi, Kayseri, Turkey
e-mail: s-unalan@erciyes.edu.tr

E. Özrahat
Department of Biosystems Engineering, Faculty of Engineering and Architecture, University of Bozok, 66200 Yozgat, Turkey

List of symbols

c_p	Specific heat of the concrete (kJ/kg K)
f	Friction coefficient
g	Gravitational acceleration (m/s^2)
h	Convection heat transfer coefficient (W/m^2 K)
k	Thermal conductivity of the concrete (W/m K)
k_{air}	Thermal conductivity of the air (W/m K)
L	Length of the concrete column and flow line (m)
n_c	Total columns number in the flat
Nu	Nusselt number
Pr	Prandtl number
q	Heat flux (W/m^2)
Q	Total heat transfer (kW)
E_{str}	The sensible thermal energy amount stored in column (kJ)
r	Radial direction
R	Radius of the air channel (m)
Ra	Rayleigh number
Re	Reynolds number
t	Time
Δt	Charging and discharging time (h)
T	Temperature (K)
ΔT	Truncation error of temperature (K)
ΔP	Pressure loss with air pipe flow rate (Pa)
V	Velocity (m/s)

Published online: 05 March 2014

e_p Surface roughness of the pipe (m)

Greek letters

α Thermal diffusivity (m/s^2)
ρ Density (kg/m^3)
β Thermal expansion coefficient (1/K)
υ Kinematic viscosity of air (m^2/s)
σ Stefan–Boltzman constant $= 5{,}67.10^{-8}$ W/m^2 K^4
ε Emissivity of the concrete surface

Subscripts

a Air
ave Averaged
c Conduction
cir Circulation
com Combined
ext External
for Forced convection
in Inlet
int Internal
m Medium
nat Natural convection
out Outlet
rad Radiation
std Steady

1 Introduction

Today, the rising energy demand is getting fulfilled by fossil energy sources (steady sources) such as natural gas, coal and petroleum and renewable energies sources (transient sources) such as solar energy, wind energy and waste energy. A significant part of total energy consumption in countries especially having cold climate is used for building heating. For the building heating process needed in certain moments of the day, the transient energies have to store as thermal energy in the various mediums. For that purpose, the buildings have to be constructed by using materials with high thermal energy storage capacity. Recently, investigation of buildings with high thermal energy storage capacity has become one of the hottest topics in thermal energy engineering and building industry. The thermal energy can be stored as latent heat with phase change materials (PCMs) and sensible heat with solid materials.

In literature, for latent heat energy storage in buildings, the use of PCMs in floors, roofs, walls, and ceiling of a building has been investigated extensively. PCMs classified as organic, inorganic and eutectic can be either used directly or by integrating with materials of construction elements. The use of PCMs are very popular in building applications such as PCM Trombe wall used as wall passive building elements which rely on solar-induced buoyancy-driven convection, PCM wallboard, PCM shutter, under-floor heating system and ceiling board. Their latent heat capacity and isothermal behavior during the phase change process have been reviewed extensively in literature [1–6]. However, the use of PCMs such as paraffin compounds, non-paraffin compounds, salt hydrates, metallics, fatty acids and eutectics suggested in previous studies are fairly expensive in terms of the building cost and is not be practical in terms of current building technology and safety. In addition, the PCMs in the building cause various problems. Paraffin shows some undesirable properties such as low thermal conductivity, non-compatible with the plastic container and moderately flammable. Non-paraffin PCMs are also flammable and should not be exposed to excessively high temperature, flames or oxidizing agents. The most important problem of salt hydrates is salt segregation and super cooling [1]. PCM incorporation methods have been considered as: direct incorporation, immersion and encapsulation [3]. First two methods are flexible and economical. However, it has been pointed out that the leakage may be a problem over the life time of many years for these two methods [7]. The third method can be defined as the containment of PCM within a capsule of various materials, forms and sizes prior to incorporation so that it may be introduced to the mix in a convenient manner. There are two principal means of micro encapsulation and macro encapsulation. Both methods of PCM encapsulation in concrete may have some drawbacks. Plastic or metallic encapsulation of the PCM is expensive but safe, as the PCM is not in contact with the concrete. Micro encapsulation by impregnating the PCM in the concrete is very effective, but it may affect the mechanical strength of the concrete [3, 5]. Therefore, the latent heat storage in the wall, beam and column with PCMs that requires special approach and production techniques could not be recommended in terms of today's conditions. Consequently, the sensible heat storage in the wall, ceiling, floor, beam and column would be more convenient if the cost and special building technology requirement considered.

Among the materials used for building technology such as iron, brick, wood, plastics, concrete and plaster, the concrete and plaster are important construction elements in terms of large mass or volume. This large mass serving higher energy storage will be an important advantage in thermal energy storage. The concrete columns with large mass constitute nearly half of the material used in a building construction. Therefore, researchers are interested in using concrete as a thermal storage medium for a long time. However, as mentioned above, most of the studies were made over latent heat storage in concrete with PCMs. Only a few studies are using concrete without PCM as a

sensible heat storage material for building heating and cooling applications. A system which is called as 'hydronic concrete core system'and which consists of a concrete slab and water pipes acts as heat accumulator and permits dissipation of the thermal loads. For instance, cooling towers, is studied in order to describe the interrelationship between heat storage capacity and pipe geometry [8]. The influence of thermal parameters affected by water circulation, flow and temperature upon the amount of stored energy was evaluated by keeping material and geometry of the prototype constant in a vertical wall made of a cellular clayey concrete which has been fitted with water pipes [9]. For a parabolic through power plant, two storage systems have been developed: a castable ceramic and a high temperature concrete. Both materials are found to be suitable for solid media sensible heat storage [10]. A mixing ventilation system characterized by the concrete slab mass activation developed through the hollow core concrete slab is compared with the traditional system and it is shown that the night ventilation, better if coupled with mass activation, can drastically help on reducing summer cooling loads and on improving thermal comfort [11]. A simplified dynamic thermal model of a hollow core concrete slab thermal storage system and associated room is described [12]. A numerical model was developed and a study was undertaken to investigate the thermal performance of various components of the TermoDeck hollow core concrete slab system defining a versatile energy storage technique for controlling the environment within large and medium sized buildings [13]. A study was carried out for the investigation of the effect of air cavities on the heat transfer behavior and diurnal heat storing capacity of the concrete slabs and for the usage of this information to create an analogous, generic 1-D model for such type of constructions [14].

In previous works, storage of sensible energy in buildings columns is not considered. Especially, storing energy in walls and floor rather than columns is studied. Walls and floor are building components in which lighter materials are used and which have more air gaps. Less mass means less energy storage potential. However, columns have large mass. Thus columns have more energy storage potential. Especially, in multi-storey buildings, great column volume and mass is attractive to be energy storage medium. In order to store more energy, using bricks and floor materials with high density can be considered. However, this approach will increase the static load of the buildings columns.

On the other hand, the sensible thermal energy storage in the horizontal components of the building except the column would also be impractical because of economical, building and health problems caused by fluid flow channel construction in these components. To introduce a channel system distributed into floors, ceilings and beams wouldn't be simple and cheap. However, the vertical channels, pipes and special pipe systems in the column can be formed easily with existing technology without affecting the building cost. In addition, heating from horizontal surfaces such as the floor is not approved because of dispersing very small dusts and microbes on the floor to all room space by natural convection flow. When compared with the traditional heater systems, the columns as a heater will have important advantages. Consequently, the main scope of this study is to investigate application of the concrete column with reinforcement as a sensible thermal energy storage medium and a heater. Thereby, the transient thermal performance would be analyzed analytically. In literature, there is no theoretical or experimental study available for the proposed system. Results obtained from this study may be of interesting for many researchers working on various fields such as heat transfer, civil engineering, thermal fatigue and medical health.

2 Problem description

In this study, storage potentials of sensible thermal energy on the concrete columns will be investigated for multi-storey buildings. Therefore, a new mission will be installed on the columns carrying of the building's static and dynamic loads. In the system, instead of traditional heating systems, a new heating system based on column surfaces is considered. Instead of the traditional concrete column, a concrete column with pipes and special pipe systems placed inside the column will be used. Schematics of the proposed system and probable heat transfer mechanisms can be seen in Fig. 1. The thermal energy from an energy center will be carried by means of dry air flowing inside pipes and special pipe systems to concrete columns. The transverse sections of pipes and special pipe systems and the possible column positions within a building can be schematically seen in Fig. 2. In order to decrease thermal energy losses, columns surfaces that are exposed to the atmosphere should be isolated. In the proposed system, the pipes and special pipe systems made of stainless steel will increase also static and dynamic strength of the concrete column. The sensible thermal energy from the energy center would initially be stored by means of forced convection in column medium. Then, while a part (q_{out}) of the stored thermal energy will transfer by natural convection and radiation from the column surface to indoor spaces, the rest (q_c) of the thermal energy in column will conduct to building elements such as wall, beam, ceiling and floor connected to the column. Thereby, the thermal energy can be stored also in other building elements. Also thermal energy conducted from columns to other building elements will also be transferred the indoor spaces by convection and radiation. The thermal energy stored in column, wall, beam, ceiling and

floor having low thermal conductivity cannot rapidly discharge to the indoor. As seen Figs. 1 and 2, the heat transferring surface with the proposed system will considerably increase according to conventional heating systems. Thus, a man in the room will expose the radiation heat flowing many directions. This will an important advantage in terms of thermal comfort. Consequently, the proposed system can be served as both the thermal energy storage medium and the room heater. In new system, the thermal energy storage process (energy charging) and room heating process (energy discharging) will occur simultaneously.

In the suggested system, an important problem will occur in terms of heating at the same rate of all floors. As seen in Fig. 1, the air circulation with individual direction

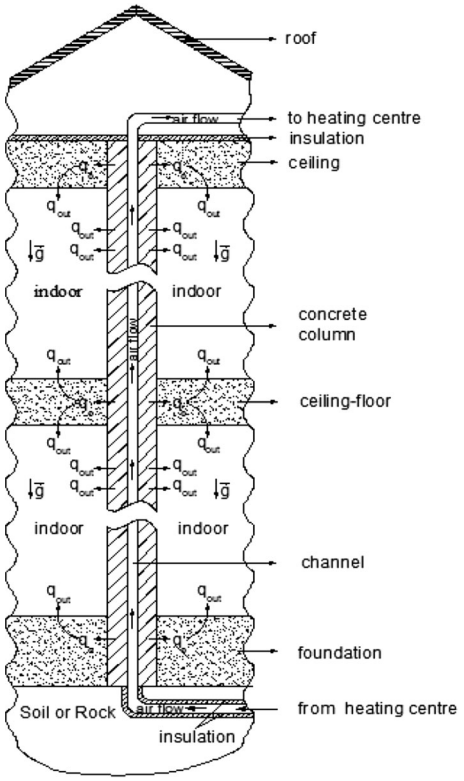

Fig. 1 Longitudinal column cross section in building

(only from bottom to roof) causes a decreasing temperature distribution versus the channel axis and lower warming of the houses in the upstairs or higher warming of the houses in the downstairs. The heated air entering with a constant inlet temperature from the heating centre will leave from other side with a transient outlet temperature. The outlet temperature will increase as a function of the charging time. However, a large temperature difference between inlet and outlet occurs. This problem can be solved by two methods. The first method is bidirectional air circulation. The air flow direction can be changed as from bottom to roof of the building and from the roof to the bottom, periodically. The temperature difference can be considerably reduced by the bidirectional air circulation. The second method can be a special system with two pipes filled with PCMs. In the special system (see in Fig. 3) working air circulation with individual direction, PCM material which has a constant melting point, will be placed between two pipes which one has small diameter and the other has bigger diameter. The dry air will flow through the pipe with small diameter. Therefore, after a certain period, as the PCM melts between the two pipes, at the interface of pipe has bigger diameter constant temperature of PCM melting point will be achieved. If dimensions of the special system, PCM layer thickness, channel length, thermal conductivity of the PCM are chosen suitably a constant temperature distribution along channel axis is possible. This result will serves heating all floors at the same rate. As a result of two ways, the temperature in the channel axis can be assumed at a constant value in the analytical calculations (see Sect. 3). While the freezing points of paraffins, as a type of PCM, is between 42 and 68 °C (315–341 K), the melting points of paraffins is between 5.5 and 75.9 °C (279–349 K). The melting points of non-paraffins is between 7.8 and 127.2 °C (281–400 K) and fatty acids is between 16.7 and 102 °C (290–375 K) [1]. Therefore, the PCM type for the special pipe system could be selected from literature for the operation temperature corresponding to the energy requirement of the houses. For a high thermal performance and a long life, the PCM in special pipe system must have a

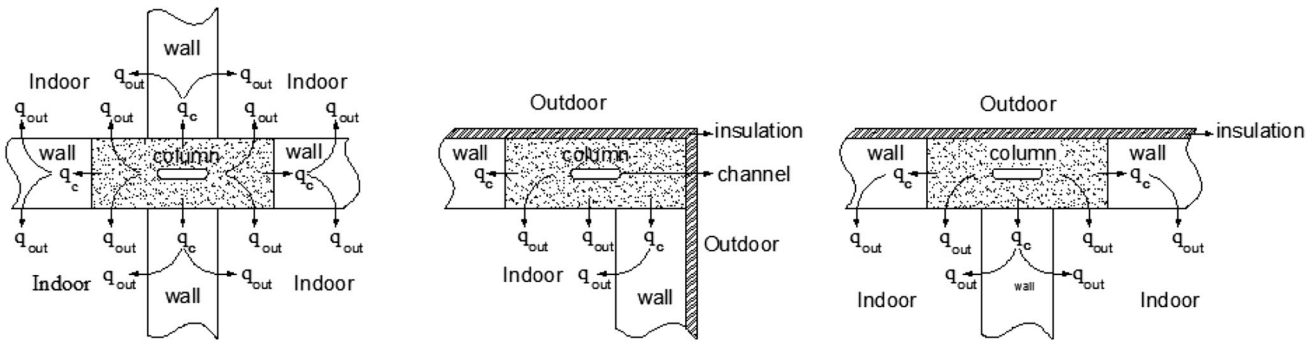

Fig. 2 Transverse column cross sections in building

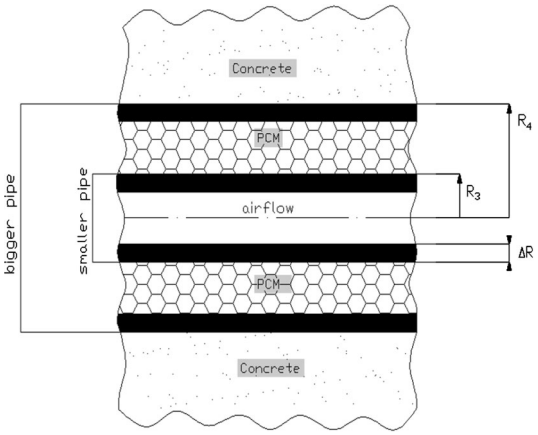

Fig. 3 The special pipe system with PCMs

high thermal conductivity, high evaporation temperature so that evaporation process not occurs and a good chemical compatibility with the pipe material.

The readers want to know advantages and disadvantages of the new system according to conventional systems. The advantages and disadvantages can be easily explained by simple engineering approaches. By comparing with the conventional system, advantages of the proposed system can be summarized as following:

- It will be a system that works more quite. The sounds of metal expansion caused by the sudden warming and the caused by the water flowing in the radiator and pipes, and noise caused by the air flowing from the fan coil systems to room medium will not occur in this system.
- Heating elements like radiator, pipe and fan coil will not occupy a place so there wouldn't be visual pollution.
- It will be a more economic system in terms of material and building cost of the heating system. In the new system, heating elements like radiator, pipe and fan coil of the traditional heating systems will not be used; therefore, the cost will decrease. However, canalization process and the use of pipes and special pipe system in the columns will bring additional cost. Consequently, cost of the new system will not be as high as traditional system.
- It will be a system which provides more natural heating. As the heating surfaces are enlarged, the heat flow to the room medium will occur gradually and continuously. There will not appear strong local air circulations that are caused by forced convection in fan coils and by a strong convection nearby the radiator which has higher surface temperature.
- It will be a more comfortable system according to the traditional systems working periodically. Generally, the traditional systems run twice as in the morning and evening through the period of 24 h. This causes greater temperature fluctuations in the room at period of 24 h. In a comfortable room the temperature should not change too much during the day. However, in the investigated system, as the thermal energy can be stored rapidly in columns, the energy discharging process from the column surfaces to room medium is slowly realized because of low thermal conductivity. In other words, the new system could be a heating system that works in an almost steady state regime. Therefore, the temperature distribution as a function of the time and space will be more uniform.

Despite the advantages that mentioned above, there are important disadvantages of the considered system. These are:

- Extra loads will be added on all building columns that carries dynamic and static loads. The first load will be thermal loads as a function of the temperature. The second load would be thermal fatigue with transient temperature variations because of cooling and heating processes to be repeated for years. The concrete losses some of the initial compressive strength with the effect of high temperatures. The reinforced concrete composed by cement, aggregate and iron with different thermal expansion coefficients will expose splits, cracks and stress concentrations. In previous study [15], it has been shown that the concrete strength losses at the temperatures above 300 °C (573 K) decreased significantly. For the current case, this temperature can be a limit.
- The volume and the indoor facing surfaces of buildings existing columns may not show enough storage performance and enough heating performance, respectively. In the considered system, structures and geometries of the existing building elements wouldn't be changed. Only to compensate the reduction in the cross-section caused by the channel gaps having an equivalent diameter of 5–10 cm in the column, existing column cross-sections would be a little larger. However, in case of stainless steel pipe instead of the channel gap, there will not occur any strength decay in the columns.

Extent of these two main disadvantages depends on the temperature values affected on the concrete columns. Without knowing the temperature distribution in the column, no provision can be given about the effects of these disadvantages. The aim of this study is to calculate the approximate transient temperature distribution providing sufficient heating for a sample building.

3 Analytical solution

In this study, the main aim is to calculate the temperature distribution as a function of the operation time and temperature ranges required for enough heating of a flat on an average column analytically. Also it is aimed to analyze the energy charging process to columns and energy discharging process from the columns to room medium. Unfortunately, all problems raised from the suggested concept cannot be addressed in this work. For general results, the analytical solutions will be performed by a simplified model. Otherwise, for the different column positions in building as shown in Figs. 1 and 2, an analytical solution considering all components cannot be performed. For the more simplified solution, plaster, iron, pipe, special pipe system, paint layer, walls and beams connected with the column are ignored in analytical solution. Therefore, the air flowing assumption at the constant temperature of T_a in the column would not be wrong and will give an important data about the air and concrete temperature ranges required for enough heating of the house. For simplicity, all sections such as the rectangular column or elliptic channels seen in the Fig. 2 was assumed to have a cylindrical geometry.

Consequently, the transient calculations in the cylindrical geometry in Fig. 4 carried out in 1-dimensional cylindrical coordinates. On the other hand, the transient thermal calculations are performed for various stages. At the first stage, the first energy charging to be realized up to the desirable energy storage level and energy discharging process will be followed by the time interval of Δt_1. At the beginning of this stage, the initial temperatures for all building components and air were assumed as a value of T_m. At the second stage, the only energy discharging process will be followed by the time interval of Δt_2. Then, the energy charging and discharging processes will be repeated by the time interval of Δt_3. The operations performed for the time intervals of Δt_2 and Δt_3 repeated periodically during all winter months. In calculations, mathematical explanation of the heat transfer rate from cylindrical surface to the room will be important. As mentioned above, all of the thermal energy stored in the columns will transfer by direct natural convection and radiation to the room atmosphere, other building elements and furniture in the house. As a function of the surface and surrounding temperatures, the heat transfer flux can be explained as follow:

$$q_{out} = q_{rad} + q_{nat} = \sigma\varepsilon\left[T_{ext}^4 - T_m^4\right] + h_{nat}[T_{ext} - T_m] \quad (1)$$

The equation is a nonlinear equation mathematically because of the radiation term. This nonlinear case as boundary condition occurs as a major difficulty on analytical solutions of the partial differential. For this reason, the radiation and convection heat transfers are combined as follow:

$$q_{out} = h_{com}[T_{ext} - T_m] \quad (2)$$

The h_{nat} natural convection heat transfer coefficient in Eq. 1 can be calculated by Eqs. 32 and 33 for certain T_{ext} and T_m values. Then h_{com} combined heat transfer coefficient can be determined from Eq. 2 for various emissivity values. For the first stage, the temperature distribution in the concrete column can be governed by following differential equation, boundary and initial conditions:

$$\frac{1}{r}\frac{\partial T}{\partial r} + \frac{\partial^2 T}{\partial r^2} = \frac{1}{\alpha}\frac{\partial T}{\partial t} \quad (3)$$

$$-k\left(\frac{\partial T}{\partial r}\right)_{r=R_{ext}} = h_{com}[T(R_{ext}, t) - T_m] \quad (4)$$

$$-k\left(\frac{\partial T}{\partial r}\right)_{r=R_{int}} = h_{for}[T_a - T(R_{int}, t)] \quad (5-a)$$

$$T(r, 0) = T_m \quad (6-a)$$

In the Eqs. 3–6, if a transformation is done as $T(r,t) = \theta(r,t) + B(r) + T_m$ and the new equations obtained with this transformation are superposed with respect to the new dependent variables (θ and B) we obtain :

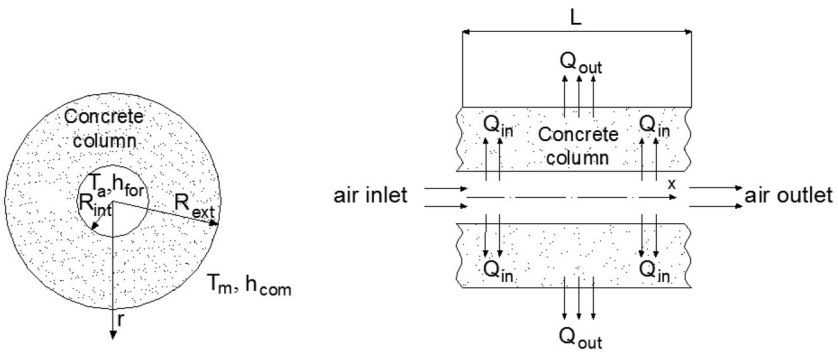

Fig. 4 Cylindrical column cross section for analytical solution

$$\frac{1}{r}\frac{\partial\theta}{\partial r}+\frac{\partial^2\theta}{\partial r^2}=\frac{1}{\alpha}\frac{\partial\theta}{\partial t} \tag{7}$$

$$-k\left(\frac{\partial\theta}{\partial r}\right)_{r=R_{ext}}=h_{com}\theta(R_{ext},t) \tag{8}$$

$$-k\left(\frac{\partial\theta}{\partial r}\right)_{r=R_{int}}=-h_{for}\theta(R_{int},t) \tag{9}$$

$$\theta(r,0)=-B(r) \tag{10}$$

$$\frac{1}{r}\frac{dB}{dr}+\frac{d^2B}{dr^2}=0 \tag{11}$$

$$-k\left(\frac{dB}{dr}\right)_{r=R_{ext}}=h_{com}B(R_{ext}) \tag{12}$$

$$-k\left(\frac{dB}{dr}\right)_{r=R_{int}}=h_{for}[T_a-T_m-B(R_{int})] \tag{13}$$

Solution of the partial differential in Eq. 7 by means of separation of variables method $[\theta(r,t)=\phi(r)\tau(t)]$ and derivation with respect to r is as follows:

$$\theta(r,t)=[C_1J_0(\lambda_n r)+C_2Y_0(\lambda_n r)]e^{-\alpha\lambda_n^2 t} \tag{14}$$

$$\frac{\partial\theta}{\partial r}=-\lambda_n[C_1J_1(\lambda_n r)+C_2Y_1(\lambda_n r)]e^{-\alpha\lambda_n^2 t} \tag{15}$$

In the above equations, J_0, J_1, Y_0 and Y_1 in Eqs. (14–15) are Bessel functions and modified Bessel functions of orders 0 and 1, respectively. By the application of the boundary conditions (8) and (9) to Eq. 14, following equations are obtained:

$$C_2=\frac{h_{com}J_0(\lambda_n R_{ext})-k\lambda_n J_1(\lambda_n R_{ext})}{k\lambda_n Y_1(\lambda_n R_{ext})-h_{com}Y_0(\lambda_n R_{ext})}C_1 \tag{16}$$

$$C_2=-\frac{h_{for}J_0(\lambda_n R_{int})+k\lambda_n J_1(\lambda_n R_{int})}{k\lambda_n Y_1(\lambda_n R_{int})+h_{for}Y_0(\lambda_n R_{int})}C_1 \tag{17}$$

By eliminating C_1 and C_2 constants between the Eqs. 16 and 17 following eigenfunction is obtained:

$$\frac{\left[k\lambda_n Y_1(\lambda_n R_{int})+h_{for}Y_0(\lambda_n R_{int})\right]\left[k\lambda_n J_1(\lambda_n R_{ext})-h_{com}J_0(\lambda_n R_{ext})\right]}{\left[h_{for}J_0(\lambda_n R_{int})+k\lambda_n J_1(\lambda_n R_{int})\right]\left[k\lambda_n Y_1(\lambda_n R_{ext})-h_{com}Y_0(\lambda_n R_{ext})\right]}=1 \tag{18}$$

λ_n eigenvalues (n = 1, 2, 3, 4, …) as positive roots of Eq. 18 can be calculated by above eigenfunction. In Eq. 16, an abbreviation as:

$$H_n=\frac{h_{com}J_0(\lambda_n R_{ext})-k\lambda_n J_1(\lambda_n R_{ext})}{k\lambda_n Y_1(\lambda_n R_{ext})-h_{com}Y_0(\lambda_n R_{ext})}, \tag{19}$$

is applied, then C_2 will be $C_2=H_nC_1$. By assuming $C_1=C_n$ and rearranging Eq. 14 we obtain:

$$\theta(r,t)=C_n[J_0(\lambda_n r)+H_nY_0(\lambda_n r)]e^{-\alpha\lambda_n^2 t} \tag{20}$$

By applying the initial condition (10) to the Eq. 20:

$$-B(r)=C_n[J_0(\lambda_n r)+H_nY_0(\lambda_n r)] \tag{21}$$

is obtained. By applying the Fourier approaches to the last equation, C_n coefficients can be calculated by the following integrals:

$$C_n=\frac{-\int_{R_{int}}^{R_{ext}}rB(r)[J_0(\lambda_n r)+H_nY_0(\lambda_n r)]dr}{\int_{R_{int}}^{R_{ext}}r[J_0(\lambda_n r)+H_nY_0(\lambda_n r)]^2dr} \tag{22}$$

The solution of ordinary differential equation in Eq. 11 with the boundary conditions (12) and (13) can be obtained easily as follows:

$$B(r)=\frac{T_m-T_a}{\frac{k}{h_{com}R_{ext}}+\frac{k}{h_{for}R_{int}}+\ln\left(\frac{R_{ext}}{R_{int}}\right)}\left[\ln\left(\frac{r}{R_{int}}\right)-\frac{k}{h_{com}R_{ext}}\right] \tag{23}$$

For the first stage indicated by I upper script, the obtained temperature distribution as a function of r-dimension and t-time by mean of separation method is as follows:

$$T^I(r,t)=\sum_{n=1}^{\infty}C_n[J_0(\lambda_n r)+H_nY_0(\lambda_n r)]e^{-\alpha\lambda_n^2 t}+B(r)+T_m \tag{24}$$

At the second stage, the air circulation in the concrete columns or the thermal energy storage processes will be stopped for time interval of Δt_2. In this case, it occurs only natural convection in the closed channels because of no air flow in the channel and therefore, the heat minor transfer between the air and the column surface can be ignored. For that purpose, some boundary and initial conditions in the above equations have to be changed by follows:

$$-k\left(\frac{\partial T}{\partial r}\right)_{r=R_{ext}}=0 \tag{5-b}$$

$$T(r,0)=T^I(r,\Delta t_1) \tag{6-b}$$

Partial differential equation in Eq. 3 can be solved by using the methods given above with the new boundary and initial conditions (5-b) and (6-b), and old boundary condition (4). For the second stage indicated by II upper script, the obtained temperature distribution with new conditions is as follow:

$$T^{II}(r,t) = \sum_{n=1}^{\infty} C_n^{II}\left[Y_0(\lambda_n r) - \frac{Y_1(\lambda_n R_{int})}{J_1(\lambda_n R_{int})} J_0(\lambda_n r)\right] e^{-\alpha\lambda_n^2 t} + T_m \tag{25}$$

where,

$$C_n^{II} = \frac{\int_{R_{int}}^{R_{ext}} r(T^I(R,\Delta t_1) - T_m)\left[Y_0(\lambda_n r) - \frac{Y_1(\lambda_n R_{int})}{J_1(\lambda_n R_{int})} J_0(\lambda_n r)\right] dr}{\int_{R_{int}}^{R_{ext}} r\left[Y_0(\lambda_n r) - \frac{Y_1(\lambda_n R_{int})}{J_1(\lambda_n R_{int})} J_0(\lambda_n r)\right]^2 dr} \tag{26}$$

λ_n eigenvalues (n = 1, 2, 3, 4, …) in the above equations can be calculated as positive roots by followed eigenfunction:

$$\frac{Y_1(\lambda_n R_{int})[k\lambda_n J_1(\lambda_n R_{ext}) - h_{com} J_0(\lambda_n R_{ext})]}{J_1(\lambda_n R_{int})[k\lambda_n Y_1(\lambda_n R_{ext}) - h_{com} Y_0(\lambda_n R_{ext})]} = 1 \tag{27}$$

At the third stage, the air circulation in the concrete columns or the thermal energy storage process will be started again for the time interval of Δt_3. In this case, the first and third stages resemble with each other except for initial condition. For that purpose, the old initial condition has to be changed by follow:

$$T(r,0) = T^{II}(r,\Delta t_2) \tag{6-c}$$

Consequently, for the third stage indicated by III upper script, the obtained temperature distribution with new conditions (6-c) is as follows:

$$T^{III}(r,t) = \sum_{n=1}^{\infty} C_n^{III}[J_0(\lambda_n r) + H_n Y_0(\lambda_n r)] e^{-\alpha\lambda_n^2 t} + B(r) + T_m \tag{28}$$

$$C_n^{III} = \frac{-\int_{R_{int}}^{R_{ext}} r(T^{II}(R,\Delta t_2) - T_m - B(r)[J_0(\lambda_n r) + H_n Y_0(\lambda_n r)] dr}{\int_{R_{int}}^{R_{ext}} r[J_0(\lambda_n r) + H_n Y_0(\lambda_n r)]^2 dr} \tag{29}$$

In the followed calculations, eigenvalues would be calculated by Eq. (18) for energy charging stages and Eq. (27) for energy discharging stages. The total heat transfer rate from all concrete columns surface to room mediums [Q_{out} (kW)] and the total heat transfer rate from the air to concrete columns [Q_{in} (kW)] versus the operation time can be calculated by following equations:

$$Q_{out}(t) = 2\pi R_{ext} n_c L h_{com}[T(R_{ext},t) - T_m] \tag{30}$$

$$Q_{in}(t) = 2\pi R_{int} n_c L h_{for}[T_a - T(R_{ext},t)] \tag{31}$$

The analyses of h_{com} are given in Sect. 4. However, the calculation equations of forced convective heat transfer coefficients (h_{for}), friction coefficient of the air flow (f) and the pressure loss with air pipe flow rate (ΔP) are as follows [16]:

$$Ra = \frac{2g[T(R_{ext},t) - T_m]L^3}{[T(R_{ext},t) - T_m]\nu\alpha_a} \tag{32}$$

$$h_{nat} = \frac{k_a}{L}\left[0.825 + \frac{0.387 Ra^{1/6}}{\left[1 + \left(\frac{0.492}{\Pr}\right)^{9/16}\right]^{8/27}}\right] \quad all\ Ra\ values \tag{33}$$

$$Re = \frac{2VR_{int}}{\nu} \tag{34}$$

$$f = \left[1.8log\left[\frac{6.9}{Re} + \left(\frac{e_p}{3.7(2R_{int})}\right)^{1.11}\right]^{-2}\right] \quad 3000 < Re < 5.10^6 \tag{35}$$

$$h_{for} = \frac{k_a}{2R_{int}}\left[\frac{\frac{f}{8}(Re - 1000)\Pr}{\left[1.07 + 12.7\left(\frac{f}{8}\right)^{\frac{1}{2}}(Pr^{2/3} - 1)\right]}\right] \quad 3000 < Re < 5.10^6 \tag{36}$$

$$\Delta P = f\frac{L}{2R_{int}}\rho_a\frac{V^2}{2} \tag{37}$$

The maximum temperature required for determination of thermal loads and thermal fatigue in the column will occur on internal surface (r = R_{int}) of the column. The maximum temperature versus operation time can be easily determined by Eq. 24 as follows:

$$T_{int}(t) = T(R_{int},t) \tag{38}$$

On the calculations formed by the above equations, there may be a discussion on the results because of the complexity and difficulty of the equations. Integrals in Eqs. (22,

26 and 29) are quite difficult and they have no analytical solutions. Because of this, integrals in these equations should be solved numerically as a function of the λ_n eigenvalues. λ_n eigenvalues will be calculated from the non-linear Eqs. (18 and 27). Also these equations need to be solved numerically. For these calculations, a packet software named MATHCAD used [17]. This software will provide convenience especially for calculations of sequential λ_n eigenvalues. MATHCAD is a packet software which can calculate mathematical operations such as derivative, integral and non-linear equation solution numerically or symbolically. It can perform a lot of mathematical operation following each other in the single worksheet, with natural mathematic notations. The natural mathematic notation means no special programming. Also it can help to draw graphs of results and to write text document in the calculation worksheet. Consequently, the calculation process will be complex. The analytical solutions of Eq. 3 with given initial and boundary conditions will be collated with the empirical equations from literature in MATHCAD. This complex calculation may cause a discussion about the results. To conclude this discussion, steady state conditions of the proposed system can be used. In this study, if the system in Fig. 4 is loaded thermal energy for a long time, temperature distribution and the heat transferred will reach to steady state condition. For the steady state case, the temperature distribution in the concrete column can be governed by following differential equation and boundary conditions:

$$\frac{1}{r}\frac{dT}{dr}+\frac{d^2T}{dr^2}=0 \tag{39}$$

$$-k\left(\frac{dT}{dr}\right)_{r=R_{ext}}=h_{com}[T(R_{ext})-T_m] \tag{40}$$

$$-k\left(\frac{dT}{dr}\right)_{r=R_{int}}=h_{for}[T_a-T(R_{int})] \tag{41}$$

By solution of above equations, the steady temperature distribution [$T_{std}(r)$ (K)] and the total heat flux [Q_{std} (kW)] values can be easily calculated as following equations:

$$T_{std}(r)=\frac{\left[\frac{k}{h_{com}R_{ext}}-\ln\left(\frac{r}{R_{ext}}\right)\right]T_a-\left[\frac{k}{h_{for}R_{int}}+\ln\left(\frac{r}{R_{int}}\right)\right]T_m}{\frac{k}{h_{com}R_{ext}}+\frac{k}{h_{for}R_{int}}+\ln\left(\frac{R_{ext}}{R_{int}}\right)} \tag{42}$$

$$Q_{std}=\frac{2\pi k n_c L[T_a-T_m]}{\frac{k}{h_{com}R_{ext}}+\frac{k}{h_{for}R_{int}}+\ln\left(\frac{R_{ext}}{R_{int}}\right)} \tag{43}$$

The most important result of the study will be the sensible thermal energy amount (E_{str}) stored in the concrete column. The energy can be calculated for the sample flat as follows:

$$E_{str}(t)=2\pi n_c L C_P\int_{R_{int}}^{R_{ext}} r[T(r,t)-T_m]dr \tag{44}$$

4 Results

The sample calculations are carried out for a building in Kayseri city of Turkey having design winter temperature of −15 °C (=258 K). The floor plan of the 11-storey building chosen for the calculations can be seen in Fig. 5. The figure give important information about heat transfer surface, positions, numbers and cross sections of the columns in the flat. Total heat requirement of a flat existing on the east-north side of the building are about 78 and 0.434 GJ for winter season and daily periods, respectively. The averaged total heat flux (Q_{ave}) for a period for the winter season of 6 months is nearby 5.3 kW. For a sufficient heating, the total heat flux of $Q_{ave} = 5.3$ kW should be conducted from all columns to indoors. As seen in Fig. 5, there are existing 14 columns ($n_c = 14$) having a total cross section area of 4.24 m^2 in each flat. The biggest and lowest column cross section areas are 0.475 and 0.25 m^2, respectively. Thereby, the thermal calculations can be performed for an averaged cylindrical column size representing for all columns. The height of the columns are L = 2.75 m and the radius of channel is chosen as $R_{int} = 0.05$ m. Appropriate to total cross section area of 4.24 m^2, the averaged radius of one column can be calculated as $R_{ext} = 0.31$ m with cylindrical column assumption $\left[\pi n_c\left(R_{ext}^2-R_{int}^2\right)=4.24\right]$. The medium temperature in the room (T_m) is assumed as 20 °C (293 K).

For various emissivity values and surface temperatures, total heat transfer rate [$=2\pi n_c R_{ext} L q_{out}$], h_{com} heat transfer coefficient and radiation heat transfer ratio in total heat rate (q_{rad}/q_{out}) calculated from Eqs. 1 and 2 can be seen in Table 1.

According to Table 1, the important part of total heat transfer rate from column surfaces was provided by the radiation heat transfer. The radiation heat transfer is higher than natural convection heat transfer. The radiation heat transfer ratio decrease with decreasing emissivity. The 5.3 kW heat flux requirement of the sample flat can be exceedingly provided by the surface temperature of 306 K. For $Q_{ave} = 5.3$ kW, the surface temperature (T_{int}) of the column and h_{com} value can be calculated as ≈303.5 K and 6.66 W/m^2 K from Eqs. 1 and 2 by means of iteration method with $\varepsilon = 0.6$, respectively. For this reason, the

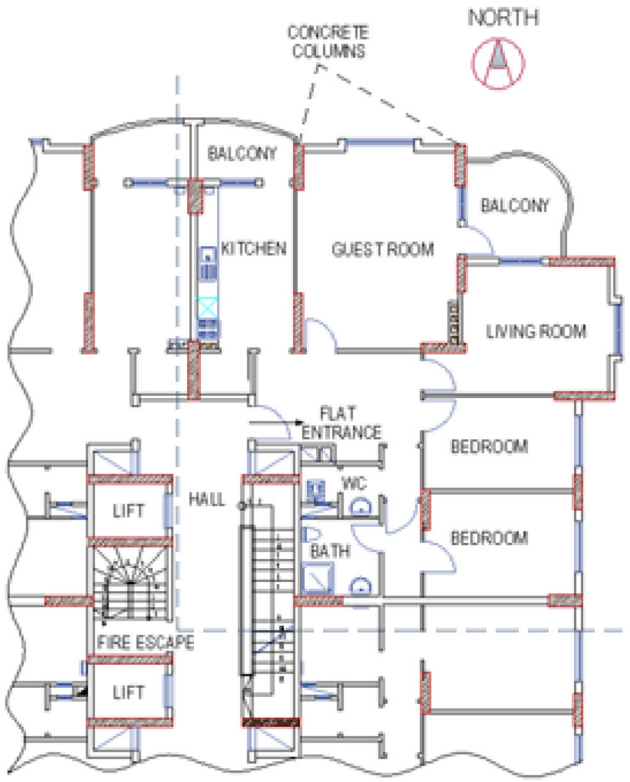

Fig. 5 Reference flats floor plan

thermo-physical properties of air in the room are taken for the temperature of 298 K corresponding temperatures of 304 and 312 K. In addition, the thermo-physical properties of air in the channel are taken for the temperature value of T_a. Preferred temperatures for T_a are between 350 and 500 K. These temperature ranges are considerably lower than the critical temperature of 573 K assumed as a limit for thermal stress and thermal fatigue problems in the literature [15]. The flow velocity (V) of the air in the channel is preferred between 1.0 and 5.0 m/s. Appropriating to these velocities, the friction coefficient (f) of air flow is calculated from Eq. 35. In these calculations, surface roughness is selected as $\varepsilon_p = 0.003$ m approximately. In addition, the air flow pressure in the channels is assumed as 3.10^5 Pa. The h_{for} values are calculated from Eq. 36 as a function of velocity, friction coefficient and pressure values in mentioned above. The pressure loss calculated from Eq. 37 with mentioned values and $L_{cir} = 60$ m can be seen in Fig. 6 for $T_a = 400$–500 K. The highest pressure loss ($\approx$1,200 Pa) occur for V = 5 m/s and $T_a = 400$ K. For investigated all cases, the pressure drop can be ignored in terms of air flow pressure of 3.10^5 Pa.

The thermo-physical properties of concrete depend on the properties of cement and aggregates [15]. In the literature, there is given different thermo-physical properties for various types of concretes. By an average approach for the concrete, the density, the thermal conductivity and the specific heat capacity is fixed as $\rho = 2{,}400$ kg/m^3, k = 2.1 W/m K and $C_p = 960$ J/kJ/kg K, respectively. All the calculations from Eqs. (1) to (43) are performed by MATHCAD [17]. All calculations are performed only for the first 500 root values of λ_n eigenvalues calculated from Eqs. (18) and (27). In this case, truncation error will be very important. Thereby, the infinite series given in Eq. (24) is truncated at $n = 500$. For V = 5 m/s and T = 500 K, the calculated eigenvalues are $\lambda_1 = 0.435898$ and $\lambda_{500} = 475.05$. The λ_n values increase with increasing given n value. Therefore, the $e^{-\alpha\lambda_n^2 t}$ term in Eq. 24 decreases by increasing λ_n value. It is obvious that for the given number of root values calculated, maximum truncation error occurs at t = 0. Therefore, the maximum truncation error can be calculated by providing that initial conditions (T(r, 0) − T_m).

$$T(r,t) = \sum_{n=1}^{500} C_n[J_0(\lambda_n r) + H_n Y_0(\lambda_n r)]e^{-\alpha\lambda_n^2 t} + B(r) + T_m + \Delta T(r,t) \quad (45)$$

$$\Delta T(r,t) = \sum_{n=1}^{500} C_n[J_0(\lambda_n r) + H_n Y_0(\lambda_n r)] + B(r) \quad (46)$$

For $T_a = 400$ K, V = 1.0 m/s and $T_a = 500$ K, V = 5.0 m/s, ΔT values calculated Eq. 46 can be seen in Figs. 7 and 8, respectively. According to these figures, the highest error obtained at the $r = R_{int}$. For $r > R_{int}$, the error

Table 1 Q_{out}, q_{rad}/q_{out} ratio and h_{com} values for various surface temperatures and emissivity values

T_{ext} (K)	Q_{out} (kW)			q_{rad}/q_{out} (%)			h_{com} (W/m^2 K)		
	ε = 0.9	ε = 0.6	ε = 0.4	ε = 0.9	ε = 0.6	ε = 0.4	ε = 0.9	ε = 0.6	ε = 0.4
295	1.03	0.79	0.62	73.8	65.70	56.15	6.872	5.264	4.106
300	4.13	3.26	2.64	66.18	57.12	47.08	7.862	6.211	5.024
305	7.64	6.11	5.02	62.97	53.68	43.60	8.476	6.779	5.565
310	11.45	9.26	7.63	61.07	51.70	41.63	8.964	7.220	5.978
315	15.51	12.54	10.44	59.83	50.43	40.37	9.384	7.592	6.321
320	19.79	16.06	13.43	58.99	49.57	39.53	9.761	7.920	6.620

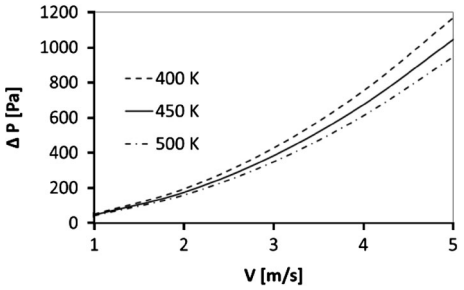

Fig. 6 Variation of pressure loss versus air velocities

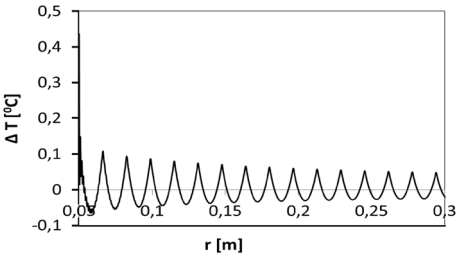

Fig. 8 Variation of ΔT versus the radius of the column for T = 500 K and V = 5 m/s

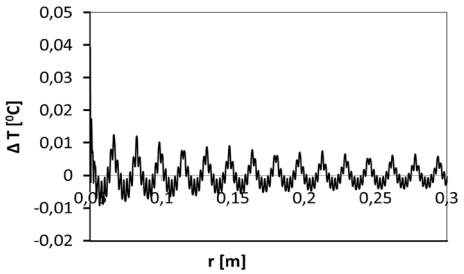

Fig. 7 Variation of ΔT versus the radius of the column for T = 350 K and V = 1 m/s

decrease rapidly. The calculated highest truncation errors are about 0.04 and 0.4 °C at the $r = R_1$, respectively. Consequently, the error results exhibited that the effect of the subsequent roots on the thermal calculations can be ignored. As mentioned in previous section, the calculations are investigated in two stages. In the first stage, for the time interval of 60 h, the first energy charging to the columns was realized. In this stage, the effects of air flow velocity (V) and temperature (T_a) on two important parameters such as Q_{out} and T_{int} are investigated as a function of the operation time (t). For each V and T_a value, the energy charging time (critical Δt_1 values) required to reach the total heat flux of $Q_{out} \approx 5.3$ kW will be determined. In the second stage, after the first energy charging of the critical Δt_1, for the various time intervals of Δt_2 and Δt_3 per 24 h ($\Delta t_2 + \Delta t_3 = 24$ h), the energy discharging and charging process will be realized periodically for 7 days. Also in this stage, Q_{out} and T_{int} will be followed according to the operation time.

Figure 9 shows variation of Q_{out} versus the operation time (t) for selected V and T_a values. Generally, the Q_{out} values behave asymptotically for $t > 60$ h. For the very long operation, the calculated Q_{out} values reach the asymptotic values represented steady state values (Q_{std}) that can be calculated from Eq. 43 for the investigated problem. For V = 1 m/s, $T_a = 350$ K and V = 5 m/s, $T_a = 450$ K, while the Q_{out} values are 6.36 and 24.46 kW at the end of charging of 60 h, the Q_{std} values are 6.40 and 24.49 kW, respectively. These results show that difficult Eqs. (1–31) used in the calculations are giving reliable results. According to Fig. 9, as expected, the critical Δt_1 values required for $Q_{out} \approx 5.3$ kW decreased with increasing of V and T_a values. For V = 1 m/s and $T_a = 350$ K, the energy charging process of $\Delta t_1 = 23$ h is not enough in terms of desired heating conditions. However, for V = 5 m/s and $T_a = 350$ K, the charging process of $\Delta t_1 = 10$ h is enough. The shortest storing time is nearly $\Delta t_1 = 4.5$ h for V = 5 m/s and $T_a = 450$ K. Generally, Fig. 9 indicates that the total heat flux of $Q_{out} \approx 5.3$ kW required for sample flat can be easily provided by $V > 1$ m/s and $T_a > 350$ K. In application of columns in the Fig. 2, the value of $Q_{out} \approx 5.3$ kW calculated for $V > 1$ m/s and $T_a > 350$ K will decrease considerably because of the negative effects of construction elements that ignored in the calculations such as plaster, paint, iron, wall, ceiling, steel pipes and of cylindrical column assumption. However, this decrease will not occur in between ranges of 100–200 % and, will be easily controlled by means of increments in the Δt_1, V and T_0 values. For example, at the end of 23 h with V = 1 m/s and $T_a = 350$ K, if the real Q_{out} is 2.65 kW with a decrease of 50 % because of the above mentioned effects, V and T_a values could be selected as 5 m/s and 450 K for the first energy charging of 7.5 h, 2 m/s and 450 K for the first energy charging of 10 h, 5 m/s and 400 K for the first energy charging of 11 h given heat flux of $Q_{out} = 10.6$ - kW, respectively. By attention to the Fig. 9, in the first 3 h, Q_{out} values are about zeros. In this period, the thermal energy is stored in the column. In other words, fast heating process for a building is not possible with the considered system. According to another result deducted from Fig. 9, the heat transferred to the room medium do not change so much when the air flow velocity is selected greater than 5 m/s. In engineering applications, the fluid flows with high velocity are not preferred because of high pressure losses and higher pumping requirement. However, as seen in Fig. 6. The highest pressure loss is ≈1,200 Pa for the

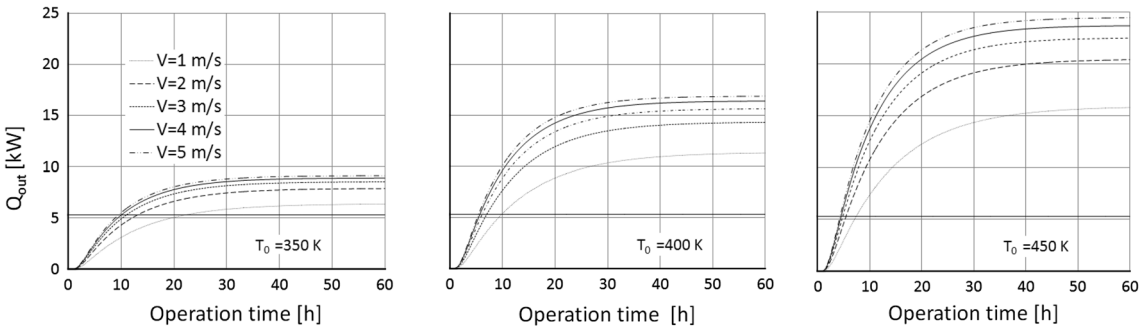

Fig. 9 Variation of Q_{out} versus the operation time

investigated cases. Another important parameter in the investigated system will be operation temperatures. For the lower thermal damage and thermal fatigue in the column, the operation temperature should be as low as possible. Consequently, the selected values for periodical charging and discharging calculations in this study would be $T_a = 360$ K, $V = 4$ m/s in terms of low temperature and high flow rate and $T_a = 400$ K, $V = 2$ m/s in terms of high temperature and low flow rate.

Figure 10 shows maximum temperature occurred in the column versus the operation time. The maximum temperature (T_{int}) in the column occurs in the columns internal surface at the inlet ($r = R_{int}$). Generally, as Fig. 9, also the T_{int} values rise rapidly to the asymptotic values (or the steady state temperatures) and then they behavior asymptotically for $t > 40$ h. For $T_a = 350$, 400 and 450 K and $V = 5$ m/s, the calculated T_{int} values are nearly 344, 388 and 430 K at the end of 60 h, respectively. Also $T_{std}(R_{int})$ values the from Eq. (42) are 344, 388 and 430 K, respectively. These temperature values are important in terms of validation of the results. On the other hand, at the end of charging process of 60 h, the highest temperature is calculated as 430 K. With $T_a = 360$ K, $V = 4$ m/s and $T_a = 400$ K, $V = 2$ m/s selected for the sample flat in Fig. 5, T_{int} decrease to $\approx$350 and 375 K at the end of charging process of 60 h. The calculated values will be reasonable for sake of concrete safety, if it is considered that the concrete are exposed to high temperatures of 420–470 K in ready mixed concrete technology for improving strength of the concrete structures, [15]. According to initial temperature of 293 K, the temperature of 375 K indicates a temperature increment of $\approx$100 K. On the other hand, in the application, the reel concrete temperatures could be higher than 375 K because of assumptions mentioned in Sect. 4. Thereby, the temperature increment value would be higher than 100 K because of the additional thermal resistance caused of construction elements that ignored in the calculations such as plaster, paint, iron, wall, ceiling, steel pipes and the effect of cylindrical column assumption instead of rectangular section. The high thermal resistance will cause higher air flow temperature for the heat requirement of building. However, the increment of $\approx$280 K (=573–293) seems impossible also in the worst case. The T_{int} will not be higher than 475 K for a temperature increment of 200 K with a deviation assumption of 100 %. In also the worst approach, the maximum temperature in the column cannot reach to 573 K.

Consequently, a danger from high temperature inside the column is not expected. On the other hand, in the literature there is no satisfying study on the thermal fatigue caused by repeated heating–cooling cycle for years in these temperature ranges. Considered that the life of a building is 50 years, it is needed to investigate the results of heating–cooling cycle going on for 50 years. For the high thermal fatigue, the sudden cooling–heating process occurs in the high temperature differences in very short time. Thereby, for the heating–cooling operations in low temperature ranges and long time periods for a day investigated in this study, an important thermal damage should not be expected. Anyway, this problem should be investigated in future.

The important parameter is external temperatures of columns. The temperature of columns surfaces heating the room medium will be important in terms of thermal comfort and health. Figure 11 shows the external temperature occurred in the column versus the operation time. The surface temperature (T_{ext}) in the column occurs in the columns external surface at the $r = R_{ext}$. Generally, as Figs. 9 and 10, also the T_{ext} values rise rapidly to the asymptotic values. For $T_a = 350$, 400 and 450 K and $V = 5$ m/s, the calculated T_{ext} values are nearly 310, 325 and 340 K at the end of 60 h, respectively. For an operation period of 10 h, these values decrease to $\approx$305, 312 and 320 K, respectively. The last values are lower than a radiator surface temperature of $\approx$340 K. Consequently, the suggested system will not rise an important problem in terms of high external surface temperature.

Figure 12 indicates variation of the Q_{out} versus the operation time during the discharging process of $\Delta t_2 = 48$ h following the first storage time of $\Delta t_1 = 8$ h

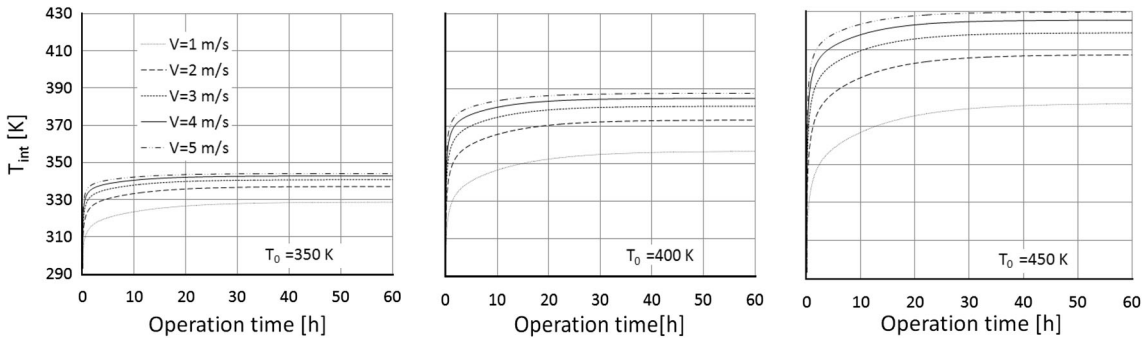

Fig. 10 Variation of T_{int} versus the operation time

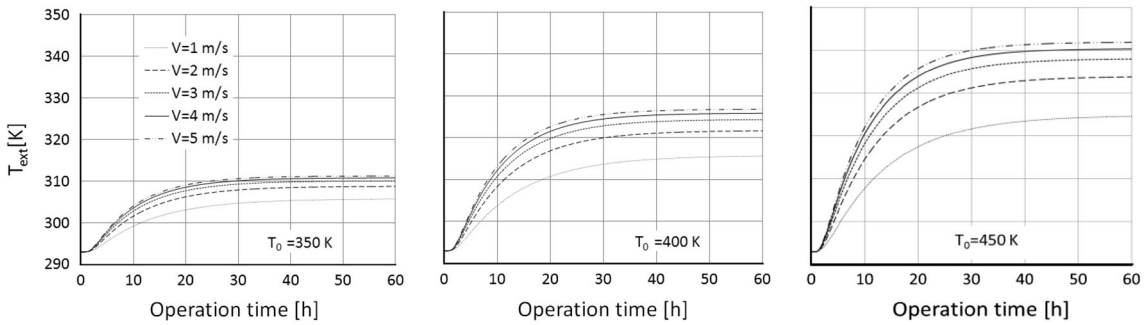

Fig. 11 Variation of T_{ext} versus the operation time

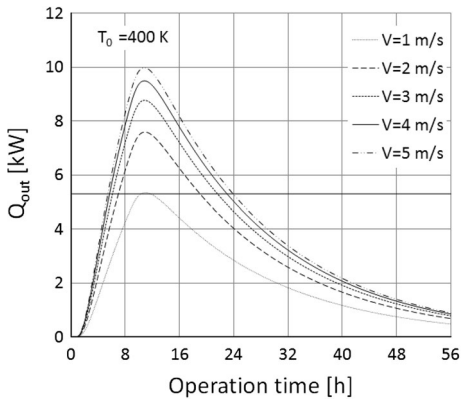

Fig. 12 Variation of Q_{out} versus operation time

for $T_a = 400$ K. According to this figure, the energy charged in short time can be discharged in a longer time period. This means that the stored thermal energy in the concrete column could be used in the flat heating process for a few days. In this case, indoor that can take energy from column by natural convection and radiation will stay nearby a specific temperature.

One of the aims of this study is to store the sensible thermal energy in the concrete column. Figure 13 exhibited the sensible thermal energy stored in the concrete column versus operation time. According to these figures, the daily energy requirement of 0.434 GJ of the sample flat can be provided after an operation of 23 and 2 h for $T_a = 400$ K, $V = 1$ m/s and $T_a = 500$ K, $V = 5$ m/s, respectively. These results compatible with results from Fig. 9 show that the suggested system is applicable in practice.

In the proposed system, the energy is both stored and heated room medium. In this case, Q_{out}/Q_{in} ratio versus the operation time will be an important parameter in terms of the storage and heating performances. $Q_{out}/Q_{in} = 0$ means all energy entered the concrete column is stored, $Q_{out}/Q_{in} = 1$ means all energy entered to column is transferred to the room and no storage of the energy, $Q_{out}/Q_{in} = 0.5$ means half of the energy entered the concrete column is stored and the other half is transferred to the room medium for heating. Figure 14 shows the variations of Q_{out}/Q_{in} versus the operation time for $T_a = 350$ K. This figure is acceptable also for the other T_a values with a little deviation. According to these curves, the thermal energy storage process of the concrete column is going on for a time period over 40 h. In addition, the effect of flow velocity on this ratio can be negligible.

In the real applications, the thermal energy cannot be stored continuously. While the energy can be stored in a particular time of a day (Δt_2), heating process should happen during all the day ($\Delta t_2 + \Delta t3 = 24$ h). In the other

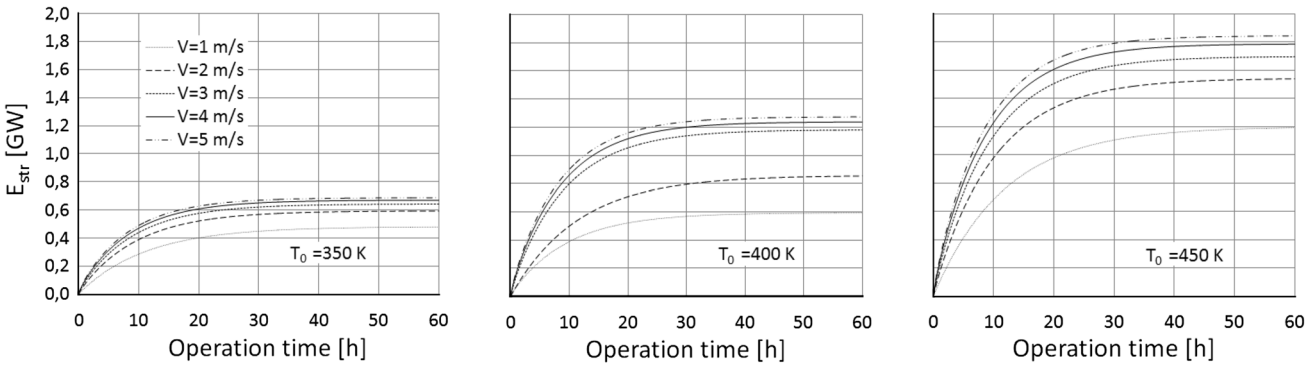

Fig. 13 Variation of E_{str} versus the operation time

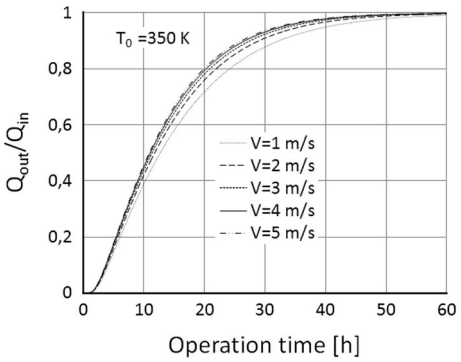

Fig. 14 Variation of Q_{out}/Q_{in} versus the operation time

word, charging and discharging process will go on for days periodically. As mentioned above, it is indicated that periodic charging and discharging analyses will be done for three models providing energy requirement of 5.3 kW cases as a result of Fig. 9. For Case-1 ($T_a = 392$ K and $V = 2$ m/s), Case-2 ($T_a = 355$ K and $V = 5$ m/s) and Case-3 ($T_a = 352$ K and $V = 3$ m/s), Figs. 15, 16, 17 and 18 show the variations of Q_{out}, T_{int}, Q_{in} and T_{ext} versus the operation time for periodic discharging (cooling) and charging (heating) processes of $\Delta t_2 = 18$, 16 and 14 h (the night) and $\Delta t_3 = 6$, 8 and 10 h (the day) hours during process of 7 days after the first storage of $\Delta t_1 = 8$, 16 and 24 h, respectively. In addition, for investigated air velocities, T_a values providing the averaged energy requirement of 5.3 kW can be seen in Table 2. At this point it should be indicated that Figs. 15, 16, 17, and 18 are showing the curves obtained for three cases (Case-1, Case-2 and Case-3) choosen from Table 2. For the same Δt_1 and Δt_2 same curves are obtained with a small deviation. Thus, all the cases of Table 2 are not expressed by figures. The most important result obtained from these figures and table is that, in a day period, the heat amount transferred into room medium can be controlled also by Δt_1, Δt_2 and Δt_3 such as T_a and V values. The effects of the first storage on the Q_{out}, Q_{in}, T_{int} and T_{ext} values diminish with increasing operation time. After a few days than the first storage process, the new Q_{out}, Q_{in}, T_{int} and T_{ext} equilibriums occur as a function of Δt_2 and Δt_3 values. In addition, the occurred results are answering the question how the thermal comfort wanted by humans can be provided. Energy storage processes should be started before 3–5 h than the coldest time of the day. After the operation of 48 h, Fig. 15 indicates that the averaged Q_{out} value is remaining $\approx$5.3 kW during 5 days. These results show that the considered system can meet the heating requirement for days after the first charging of 6, 8 and 10 h. However, according to Fig. 15, it is obvious that enough heating performance is not provided in first 2 days. This deficiency can be eliminated by increasing the values of Δt_1. In the models mentioned above, by taking $\Delta t_1 = 8.35$, 11 and 13.65 h only Q_{out} values are obtained in Fig. 15b, respectively. Figure 15b is showing that by increasing 2–3 h of the first charging period, enough heating will occur in first 2 days. According to Fig. 17, the temperature distribution at the first stages of discharging and charging processes exhibited very high gradients. This may be a very important problem in terms of thermal fatigue and thermal stress values of the concrete. In this point, it should be remembered that the heating and cooling rate values play important role on the thermal fatigue and thermal stress values. In this study, for simplifying analytical solution, it is assumed that the heated dry air was given directly in the channels and the circulating process cut off suddenly. Thereby, the temperature curves with hard gradients in Fig. 17 could be observed. However, this problem can be considerably decreased by means of slowly heating and cooling processes of the circulated air at the startup and the finish, respectively. Figure 18 show that the external temperature will $\approx$303 K during operation period. Consequently, Figs. 15, 16, 17, and 18 and Table 2 show that the new approach exhibited in this study can be applied.

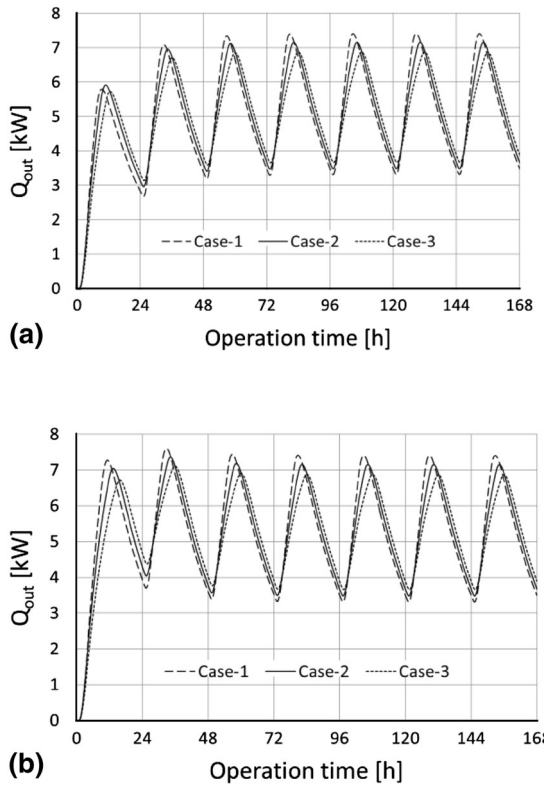

Fig. 15 Variation of Q_{out} versus operation time for different cases; [Case-1 ($V = 2$ m/s, $T_a = 392$ K, $\Delta t_3 = 6$ h), Case-2 ($V = 5$ m/s, $T_a = 355$ K, $\Delta t_3 = 8$ h) and Case-3 ($V = 3$ m/s, $T_a = 352$ K, $\Delta t_3 = 10$ h)]. **a** Case-1 ($\Delta t_1 = 6$ h), Case-2 ($\Delta t_1 = 8$ h) and Case-3 ($\Delta t_1 = 10$ h). **b** Case-1 ($\Delta t_1 = 8.35$ h), Case-2 ($\Delta t_1 = 11$ h) and Case-3 ($\Delta t_1 = 13.65$ h)

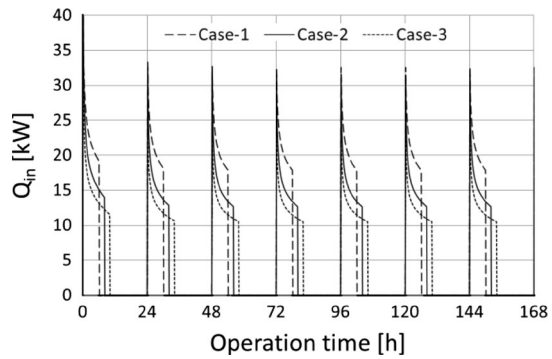

Fig. 16 Variation of Q_{in} versus the operation time for different cases; [Case-1 ($V = 2$ m/s, $T_a = 392$ K, $\Delta t_1 = \Delta t_3 = 6$ h), Case-2 ($V = 5$ m/s, $T_a = 355$ K, $\Delta t_1 = \Delta t_3 = 8$ h) and Case-3 ($V = 3$ m/s, $T_a = 352$ K, $\Delta t_1 = \Delta t_3 = 10$ h)]

5 Conclusions and recommendations

This study investigated storage possibility of sensible thermal energy in the concrete columns of multi-storey buildings and the heating performance of the indoor

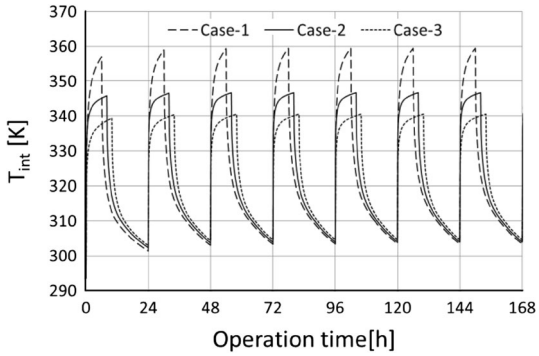

Fig. 17 Variation of T_{int} versus the operation time for different cases; [Case-1 ($V = 2$ m/s, $T_a = 392$ K, $\Delta t_1 = \Delta t_3 = 6$ h), Case-2 ($V = 5$ m/s, $T_a = 355$ K, $\Delta t_1 = \Delta t_3 = 8$ h) and Case-3 ($V = 3$ m/s, $T_a = 352$ K, $\Delta t_1 = \Delta t_3 = 10$ h)]

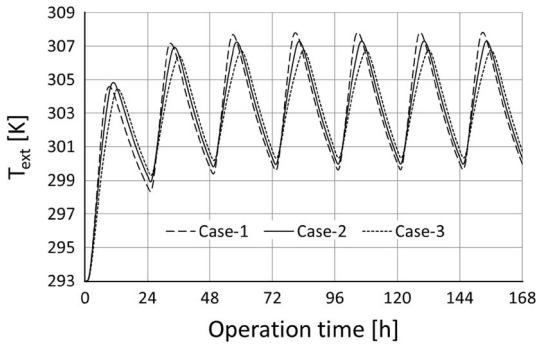

Fig. 18 Variation of T_{ext} versus the operation time for different cases; [Case-1 ($V = 2$ m/s, $T_a = 392$ K, $\Delta t_1 = \Delta t_3 = 6$ h), Case-2 ($V = 5$ m/s, $T_a = 355$ K, $\Delta t_1 = \Delta t_3 = 8$ h) and Case-3 ($V = 3$ m/s, $T_a = 352$ K, $\Delta t_1 = \Delta t_3 = 10$ h)]

Table 2 Ta (K) values providing the averaged energy requirement of 5.3 kW

V (m/s)	$\Delta t_1 = 6$ h $\Delta t_2 = 18$ h $\Delta t_3 = 6$ h	$\Delta t_1 = 8$ h $\Delta t_2 = 16$ h $\Delta t_3 = 8$ h	$\Delta t_1 = 10$ h $\Delta t_2 = 14$ h $\Delta t_3 = 10$ h
1	441	405	384
2	392	372	359
3	378	362	352
4	372	358	348
5	369	355	346

atmosphere with the stored energy. In the investigated system, the hot dry air is circulated in pipes or special pipe system passing through columns made of stainless steel. Therefore, all building columns that carry dynamic and static loads were exposed to extra loads such as thermal stresses and thermal fatigues as a function of the temperature in the column. Thereby, the main scope of this study

is to discuss the thermal performance and the temperature distribution of the concrete column with reinforcement used as the sensible thermal energy storage medium and the heater. For simplifying the analytical calculations, the transient calculations are performed over a cylindrical concrete column without plaster, iron, pipe, special pipe system, paint layer, wall and beam connections.

The sample calculations are carried out for a flat of the 11-storey building in Kayseri city of Turkey having design winter temperature of 258 K. The cylindrical column sizes are calculated as $R_{int} = 0.05$ m, $R_{ext} = 0.31$ m by means of averaged value of real column sections (14 columns with height of $L = 2.75$ m) of the selected building. The averaged energy requirement of the mentioned flat for the winter season of 6 months is nearby 5.3 kW. The temperatures (T_a) of the air flow in the channels are preferred as 350, 400 and 450 K, which are considerably lower than the critical temperature of 573 K assumed as a limit for thermal stress and thermal fatigue problems in the literature [15]. The flow velocity (V) of the air in the channel is varied between 1.0 and 5.0 m/s. For transient calculations, the initial temperature and the indoor temperature is assumed as 293 K. Consequently, for $V = 1.0$ m/s and $T_a = 350$ K, after the first charging process of 23 h, total heat flux from the column surfaces into indoor can pass beyond the value of 5.3 kW. For $T_a = 350$ K and $V = 5.0$ m/s, the first storage operation decrease 10 h. Also for $V = 5.0$ m/s and $T_a = 450$ K, the required charging time is 4.5 h. With periodic discharging of 16 h (the night) and charging of 8 h (the day) during process of 7 days, the heating requirement can be provided for $V = 1.0$ m/s and $T_a = 405$ K and $V = 5.0$ m/s and $T_a = 355$ K, after the first storage of 8 h. Consequently, a danger from high temperature inside the column is not expected. On the other hand, in the literature there is no satisfying study on the thermal fatigue caused by repeated heating–cooling cycle for years in these temperature ranges. Considered that the life of a building is 50 years, it is needed to investigate the results of heating–cooling cycle going on for 50 years. In addition, the calculations are based on a cylindrical column assumption in the cylindrical coordinate with 1-dimensional and time dependent. In the approximate calculations, other building structure elements such as plaster, paint, iron, wall, ceiling steel pipes, walls and beams connected with the column are ignored. Thereby, for more real and reliable results, the future studies have to include numerical calculations with 2 or 3-dimensionals considering these structure elements.

Acknowledgments This work is supported by the Research Fund of the Erciyes University through project number: FBA-09-869.

References

1. Sharma A, Tyagi VV, Chen CR, Buddhi D (2009) Review on thermal energy storage with phase change materials and applications. Renew Sustain Energy Rev 13:318–345
2. Zhu N, Ma Z, Wang S (2009) Dynamic characteristics and energy performance of buildings using phase change materials: a review. Energy Convers Manag 50:3169–3181
3. Pasupathy A, Velraj R, Seeniraj RV (2008) Phase change material-based building architecture for thermal management in residential and conversial establishments. Renew Sustain Energy Rev 12:39–64
4. Tyagi VV, Buddhi D (2007) PCM thermal storage in buildings: a state of art. Renew Sustain Energy Rev 11:1146–1166
5. Khudhair AM, Farid MM (2004) A review on energy conservation in building applications with thermal storage by latent heat using phase change materials. Energy Convers Manag 45:263–275
6. Farid MM, Khudhair AM, Razack SAK, Al-Hallaj S (2004) A review on phase change energy storage: materials and applications. Energy Convers Manag 45:1597–1615
7. Schossig P, Henning HM, Gschwander S, Haussmann T (2005) Micro-encapsulated phase-change materials integrated into construction materials. Sol Energy Mater Sol Cells 89(2–3):297–306
8. Koschenz M, Dorer V (1999) Interaction of an air system with concrete core conditioning. Energy Build 30:139–145
9. Marmoret L, Glouannec P, Douzane O, t'Kint de Roodenbeke A, Queneudec M (2000) Use of a cellular clayey concrete for a wall specially fitted with water pipes. Energy Build 31:89–95
10. Laing D, Steinmann WD, Tamme R, Richter C (2006) Solid media thermal storage for parabolic trough power plants. Sol Energy 80:1283–1289
11. Corgnati SP, Kindinis A (2007) Thermal mass activation by hollow core slab coupled with night ventilation reduce summer cooling loads. Build Environ 42:3285–3297
12. Ren MJ, Wright JA (1998) A ventilated slab thermal storage system model. Build Environ 33:43–52
13. Barton P, Beggs CB, Sleigh PA (2002) A theoretical study of the thermal performance of the ThermoDeck hollow core slab system. Appl Therm Eng 22:1485–1499
14. Zhang ZL, Wachenfeldt BJ (2009) Numerical study on the heat storing capacity of concrete walls with air cavities. Energy Build 41:769–773
15. Bingöl AF, Gül R (2009) A reassessment on the bond strength between reinforcement and concrete and the effect of high temperatures on the concrete and on the bond between concrete and reinforcement. Turk Sci Res Found 2(2):211–230. Available at http://www.dergi.tubav.org.tr, 2012
16. Incropera FP, DeWitt DP (1996) Fundamentals of heat and mass transfer. Wiley, Hoboken
17. MATHCAD (2012) MathSoft Inc., 101 Main Street, Cambridge, Massachusetts, 02142 USA. Available at http://www.ptc.com/products/mathcad/